Reconsideration of Design Criteria for High-Heat-Load Components at SPring-8 Front Ends

Sunao Takahashi [1], Tetsurou Mochizuki [1], Mutsumi Sano [1], Atsuo Watanabe[1], and H. Kitamura[1,2]
1 SPring-8/JASRI, 1-1-1 Kouto, Sayo, Hyogo 679-5198, Japan
2 SPring-8/RIKEN, 1-1-1 Kouto, Sayo, Hyogo 679-5198, Japan

Abstract

Elastic-plastic analysis for a real component of an absorber has been performed as part of the reconsideration of the design criteria for high-heat-load components in SPring-8 front ends. Temperature-dependent material tests for GlidCop were carried out for accurate estimation from the viewpoints of both thermal and mechanical properties. In particular, the difference of 200°C and 400°C in the low-cycle-fatigue property is noteworthy. On the basis of the cumulative linear damage low, the fatigue life of the absorber was predicted for each heat load in the range from 20 to 60 W/mm^2. According to this preliminary prediction, the fatigue life is estimated at more than 10,000 cycles when the effective peak power density is less than 50 W/mm^2, which corresponds to around three times the present limitation. The creep-fatigue interaction and demonstration of the fatigue fracture test will be presented in our next study.

1. Motivation

Although high-heat-load components (HHLCs) in SPring-8 front ends have performed satisfactorily for more than eight years, there has been a progressive increase in the heat load with the advancement of insertion devices. Moreover, there is a plan to construct a new beamline in a long-straight section whose front end will be subjected to 3.5 MW/mrad^2 with a total power of more than 50 kW.

In order to deal with this situation, we are committed to a reconsideration of the design condition for HHLCs because the design criterion for the thermal stress is believed to be too conservative. At present, the design is restricted in only the elastic deformation region. Moreover, the allowable stress is set at less than the yielding point, although the thermal stress is the secondary stress. For example, in the case of a high-pressure vessel regulated by an ASME standard, the allowable stress for the secondary stress is set at a value less than the ultimate tensile strength or twice the yield stress, whichever is less. This regulation is based on the concept that a local yielding phenomenon resulting from the secondary stress would not cause an instant fracture. Using this concept, we decided to extend the acceptance to a plastic deformation region. Therefore, the aim of this study is to present the actual acceptable power for each HHLC quantitatively, including low-cycle-fatigue evaluation.

2. Enforcement Plans for Each HHLC

At SPring-8, the grazed angle and volumetric heating technologies are the two major techniques to deal with the intensive heat load. The former is a conventional method with an inclined absorbing surface, an advanced material of GlidCop, and a wire coil inside the cooling channels that can deal with approximately 10 kW per meter in the light axis direction. The feature of the latter method is to dissipate a high surface heat flux into depth, utilizing a low-Z material of beryllium or graphite for the absorbing body so that the cooling ability might increase within a more compact space. For both the technologies, 1) material property tests, 2) establishment of a method to estimate the thermal limitation, 3) fracture tests, and 4) estimation for the real components are in progress. With regard to the indirect cooling technology used for filter components, we attempted to show the realistic value of a thermal contact resistance for a general bolted clamping component [1].

We have also been studying the fatigue life of beryllium windows and successfully introduced elastic-plastic analysis for fatigue life prediction [2]. Following this successful result, we shifted our focus to conventional grazed angle components made of GlidCop.

3. Material Property Tests for GlidCop

We performed thermal and mechanical property tests on the GlidCop at several temperatures. Since it is essential to prepare the actual material properties for accurate estimation, all the test pieces were heat-treated in advance so that a thermal record by a brazing in the actual manufacturing process might be considered.

3.1. Thermal property test

The thermal conductivity, thermal coefficient, thermal diffusivity, and specific heat were measured at temperatures of RT, 100°C, 200°C, 400°C, and 600°C.

3.2. Mechanical property test

A tensile test was performed in order to confirm the elastic-plastic property, and the stress-strain curve was obtained at temperatures of RT, 100°C, 200°C, 400°C, and 600°C. On the other hand, a low-cycle fatigue test was performed at temperatures of 100°C, 200°C, 400°C, and 600°C using the strain-regulation method. At each temperature, five load conditions were selected to ensure that the number of cycles to failure would fall between 100 and 10,000 because the actual heat cycle number tends to decrease due to the introduction of a top-up operation. The data were processed using the Manson-Coffin equation. Figures 1 and 2 show the typical results at a temperature of 400°C and the relationship between the total strain range and the number of cycles to failure for all temperatures, respectively. As shown in Fig.2, there is a significant difference in the total strain range between 200°C and 400°C, particularly in the low cycle region.

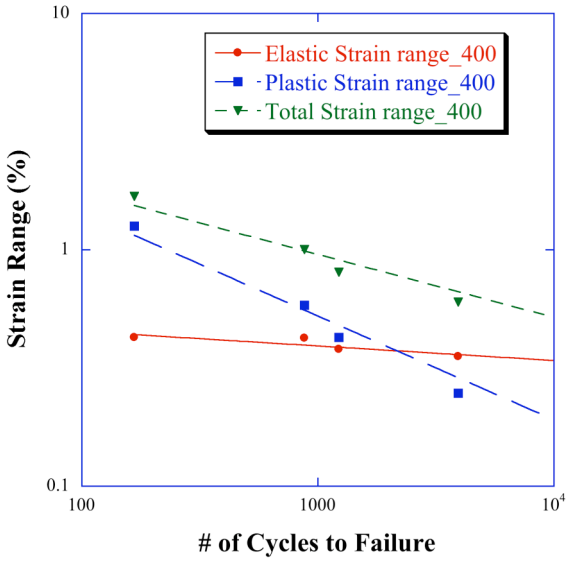

Fig. 1. Relationship between each strain range and the number of cycles to failure at a temperature of 400°C.

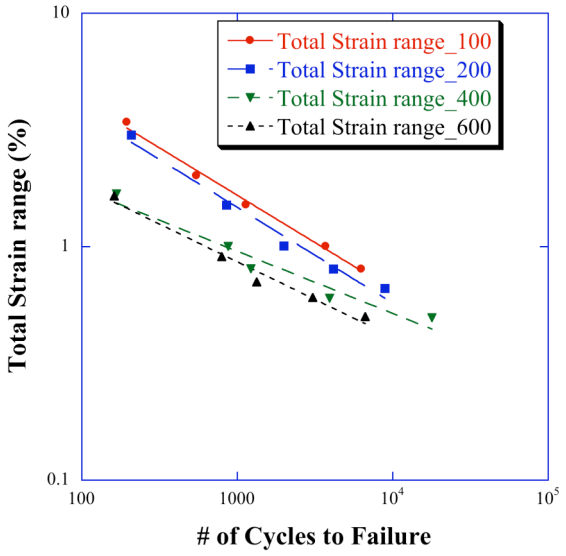

Fig. 2. Relationship between the total strain range and the number of cycles to failure at temperature of 100°C, 200°C, 400°C, and 600°C.

4. Thermal Limitation of Absorber

The absorber is one of the key components of SPring-8 front ends. As shown in Fig.3, two paths are lined up vertically inside the absorber body. The upper path of the closed mode stops the photon beam completely, whereas the lower path of the open mode passes through a fixed aperture. Each path can be moved on to the beam axis using a pneumatically driven support on which the absorber body is mounted.

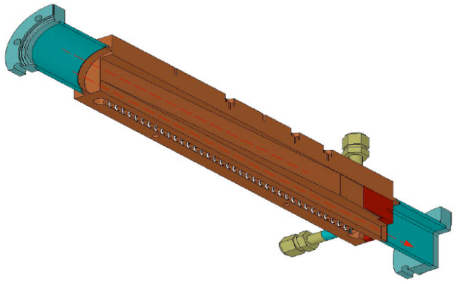

Fig. 3. Half cut section view of the model absorber.

4.1. Conventional analysis

Using the ANSYS finite element program, a conventional steady-state analysis was performed on a quarter model on the maximum heat load condition for a standard in-vacuum undulator. At the minimum insertion device gap of 8 mm, the peak power density at the absorber position reaches 1.3 kW/mm^2 with a total power of approximately 13.5 kW. Considering an inclined angle of 0.88° at the absorbing surface, the effective peak power density is estimated at 15 W/mm^2. We consider this value as a guideline for the present limitation.

Fig. 4 shows the maximum temperatures of the absorbing body and the cooling surface with an increase in the effective peak power density. Taking into account an avoidance of boiling on the cooling surface, we go ahead with elastic and plastic analysis in the range from 20 to 60 W/mm^2.

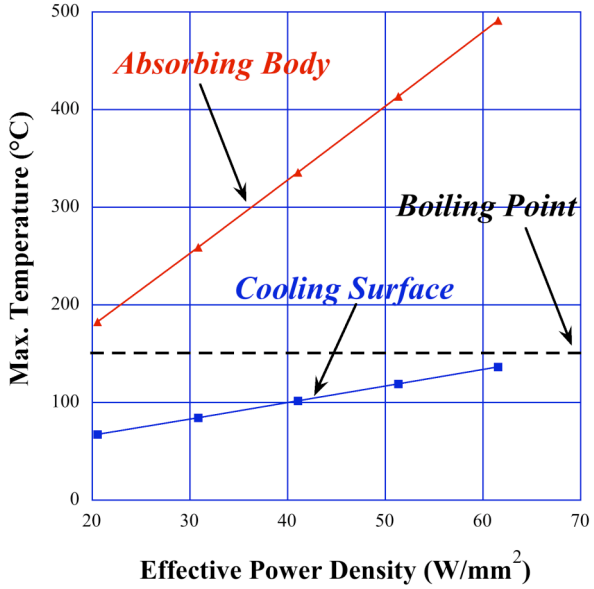

Fig. 4. Maximum temperatures of the absorbing body and cooling surface with increasing effective peak power density.

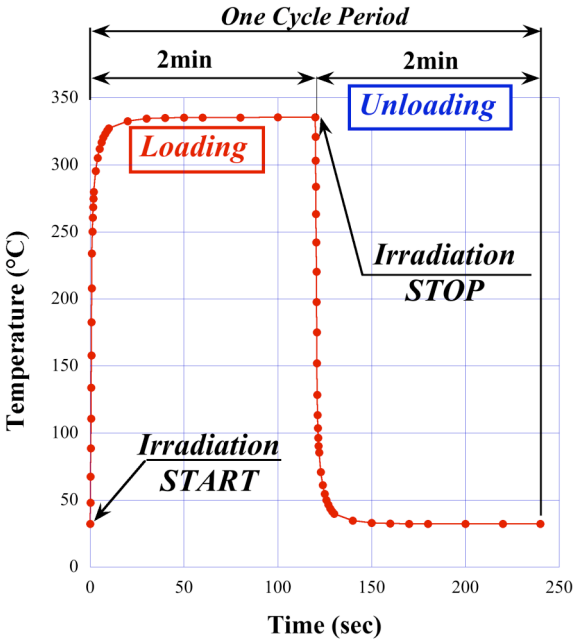

Fig. 5. Nodal solution of the maximum temperature for an absorbing body with an effective peak power density of 40 W/mm^2.

4.2. Elastic-plastic analysis

4.2.1. Preparations

A transient thermal analysis is performed for each effective peak power density. Figure 5 shows the plot of the nodal solution of the maximum temperature for the absorbing body when the effective peak power density is 40 W/mm^2. The retention time for both loading and unloading conditions is set at 2 min. We performed the five cycles in repeated succession. The temperature-dependent diagrams for the true stress and true strain, approximated by multiple straight lines, are prepared using the results of the tensile tests.

4.2.2. Results

Fig. 6(a) shows the solutions of the elastic-plastic analysis when the effective peak power density is 30.9 W/mm^2, which corresponds to twice the present maximum heat load. The cyclic diagram of equivalent stress and total strain shows an elastic shakedown. On the other hand, when the effective peak power density is greater than 40 W/mm^2, a hysteresis loop with a plastic strain range of $\Delta\varepsilon_p$ appears, as shown in Fig. 6(b). It implies that the risk of low-cycle-fatigue fracture should be examined carefully in this region.

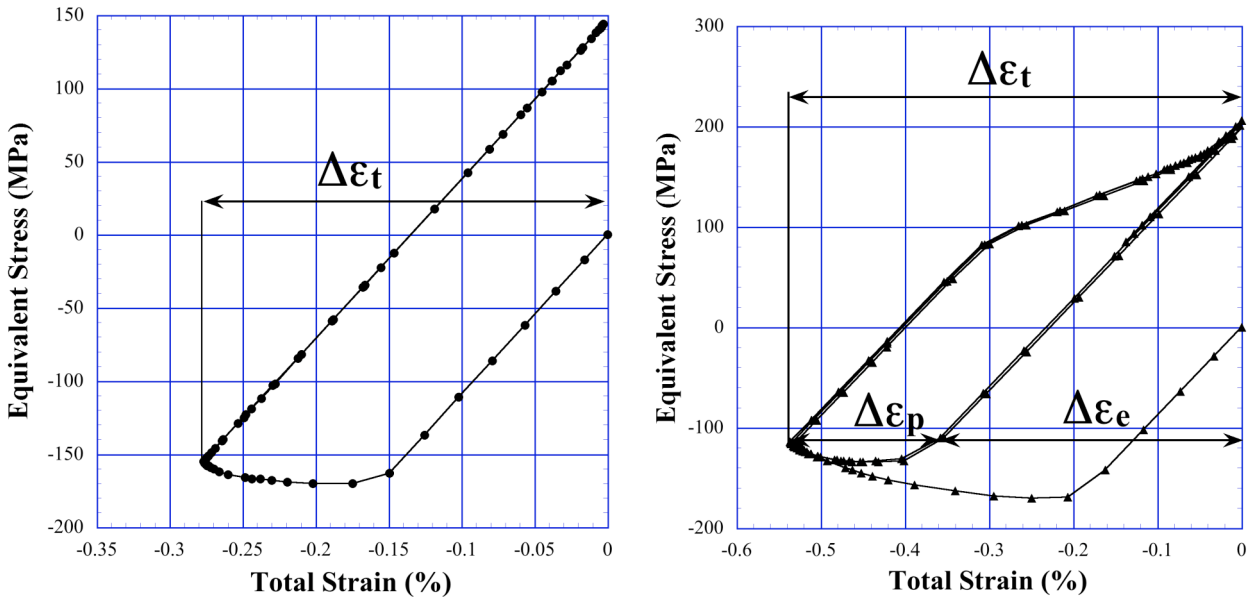

Fig. 6. Cyclic diagram of the total strain and the equivalent stress when the effective peak power density is 30.9 W/mm^2 (a) and 51.5 W/mm^2 (b), respectively.

4.3. Fatigue life prediction

The results of the total strain range were estimated on the basis of the cumulative linear damage low and given as follows:

$$\sum\left(n_i / N_i\right) = 1$$

Assuming that the number of cycles to failure is N_i at the strain range of $\Delta\varepsilon_i$, this rule considers that only one by N_i of the life of the material should be consumed in each cycle. If random heat loads similar to those that occur in the actual operation were repeated, a fracture would occur when the sum of damages for all the strain ranges becomes 1.

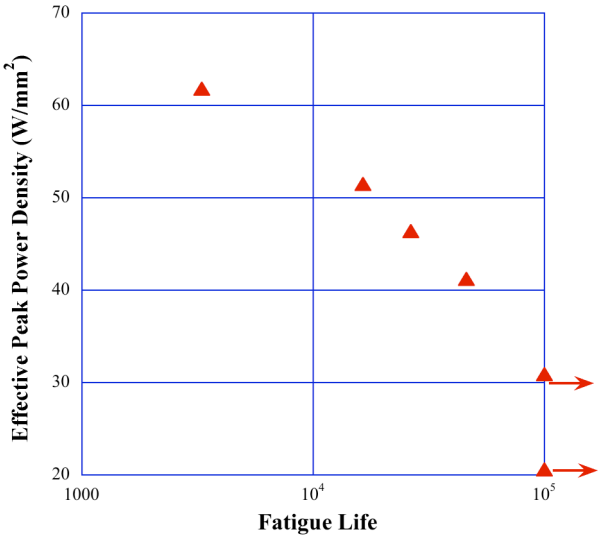

Fig. 7. Predicted fatigue life of the absorber for each effective peak power.

The predicted fatigue life of the absorber is plotted in Fig.7 as a function of the effective peak power density under the condition that the constant heat load is repeated. We select the low-cycle-fatigue data for estimation by considering the mean temperature for a high of the maximum temperature and a low of 32°C. The implications of these data are as follows:

If the allowable fatigue life is set at more than 10,000 cycles,

1) There is no problem in the case when the effective peak power density is less than 30 W/mm^2,
2) It is probably adequate in the range from 30 to 50 W/mm^2,
3) It is inadequate in the case of greater than 50 W/mm^2.

However, we should consider the fact that this guideline does not take into account the effect of creep. Generally speaking, the creep would influence a fracture at least in the range of more than approximately 300 °C, which corresponds to 0.4 times the melting point. In particular, the effect of creep becomes more important because of the top-up operation. Therefore, the creep-fatigue interaction will be investigated in our next study.

5. Conclusions and Future Work

We have successfully carried out an elastic-plastic analysis on a real component of the absorber, and introduced the cumulative linear damage low for fatigue life prediction. Consequently, the fatigue life of the absorber is estimated to be more than 10,000 cycles when the effective peak power density is less than 50 W/mm^2, which corresponds to three times the present thermal limitation. However, we should treat this estimation as a preliminary one because it does not take into account the influences of creep-fatigue interaction and the environment. We will investigate the low-cycle-fatigue property of GlidCop under the conditions of creep and vacuum.

In order to demonstrate the fatigue fracture phenomenon systematically, we will also conduct a fatigue fracture test. The objective of this test will be to predict the thermal limitation by linking analysis and experiments and to observe the progress of the fracture.

6. References

[1] M. Sano, S. Takahashi, T. Mochizuki, M. Oura, A. Watanabe, H. Kitamura, SRI2006, to be published.
[2] S. Takahashi, T. Mochizuki, H. Kitamura, MEDSI 2004 Proceedings 04-16 (2005).